Beiträge aus der Elektrotechnik

Xiao Fang

Investigation of Biomedical Antennas and Path Loss Models for Leadless Cardiac Pacemaker and Wireless Capsule Endoscopy

VOGT

Dresden 2024

Bibliografische Information der Deutschen Nationalbibliothek
Die Deutsche Nationalbibliothek verzeichnet diese Publikation in der Deutschen Nationalbibliografie; detaillierte bibliografische Daten sind im Internet über http://dnb.dnb.de abrufbar.

Bibliographic Information published by the Deutsche Nationalbibliothek
The Deutsche Nationalbibliothek lists this publication in the Deutsche Nationalbibliografie; detailed bibliographic data are available on the Internet at http://dnb.dnb.de.

Zugl.: Dresden, Techn. Univ., Diss., 2023

Die vorliegende Arbeit stimmt mit dem Original der Dissertation „Investigation of Biomedical Antennas and Path Loss Models for Leadless Cardiac Pacemaker and Wireless Capsule Endoscopy“ von Xiao Fang überein.

Gesetzt vom Autor

ISBN 978-3-95947-070-4

Jörg Vogt Verlag
Niederwaldstr. 36
01277 Dresden
Germany

Phone: +49-(0)351-31403921
Telefax: +49-(0)351-31403918
e-mail: info@vogtverlag.de
Internet : www.vogtverlag.de

TECHNISCHE UNIVERSITÄT DRESDEN

Investigation of Biomedical Antennas and Path Loss Models for Leadless Cardiac Pacemaker and Wireless Capsule Endoscopy

Xiao Fang, M. Sc.

von der Fakultät Elektrotechnik und Informationstechnik
der Technischen Universität Dresden
zur Erlangung des akademischen Grades

Doktoringenieur
(Dr.-Ing.)

genehmigte Dissertation

Vorsitzender:	Prof. Dr.-Ing. habil. Christian Georg Mayr
Gutachter:	Prof. Dr.-Ing. Dirk Plettemeier
	Prof. Narcis Cardona

Tag der Einreichung:	01. Dec. 2022
Tag der Verteidigung:	19. Dec. 2023

Acknowledgments

Pursuing the PhD degree is a long journey for me. When I first came to Germany, I didn't know what was waiting for me and how I would finish the journey. All these years' experience has enriched my life and provided me with knowledge. I would like to thank everyone who has contributed to this journey.

First, my warm thanks go to my family, my parents, wife, and son; their support always gives me the strength to overcome all the difficult situations I encountered and could not have anticipated in the long journey. Since the pandemic, I have not hugged my parents for almost four years, I miss them so much. Thank you so much for my wife, Wenjie WANG, and my son; they are the best I could have in my life, and I doubt I'd be able to complete the journey without them.

Then, I express my sincere gratitude to my supervisor, Prof. Dirk Plettemeier, who has always helped me with patience and from whom I learned a lot. And many thanks to my co-supervisors in the WiBEC project, Dr. Qiong Wang and Prof. Niels Neumann. Their expert experience in the field of body area communication has saved me a lot of detours in my research. I also thank all the members of the Chair of Radio Frequency and Photonics Engineering, who treat me so nice.

Last but not least, I would like to thank all the projects and

funding, including WiBEC, MEDICOS, and 6G Life, that have supported me to finish the thesis. Especially everyone in the WiBEC project, with whom we have done plenty of great cooperation and joint research, Mehrab, Sofia, Mirko, Faheem, Pengfei, Rafael, Martina, Salman, Deepak, Giulia, Pritam, Mohammad, Reinier, Andrea, and all the supervisors.

Abstract

The development of wireless technologies for implantable devices can contribute to improvements in the quality and efficacy of healthcare. Leadless Cardiac Pacemaker (LCP) and Wireless Capsule Endoscopy (WCE) are two state-of-the-art implantable devices that have a high potential to enable medical professionals to gather timely clinical information, increase the survival rates of the patients, relieve the pain caused by surgery, and provide other benefits. Designers of a wireless communication system for the LCP and WCE face many crucial challenges, such as the operating frequency band selection, wave propagation inside the human body, path loss models, high-efficiency and miniaturized implantable antennas, the influence of human tissues on the implantable antenna, and high gain on-body antennas.

The focus of this research was the development of stable, low-power-consumption, high-efficiency transmission links for the communication systems of LCP and WCE by building path loss models and designing novel in-body and on-body antennas. Path loss models based on practical application scenarios of LCP and WCE were built in this dissertation, and miniaturized, and highly radiation-efficient implantable antennas with new design concepts were proposed. In comparison to existing path loss models and antennas, the built path loss models excluded the effects of antenna types in all potential narrow frequency bands, whereas a comprehensive equation is proposed to simplify the process of building path loss models in the 2.4 GHz Industrial, Scientific, and Medical (ISM) band. Several new design concepts are pro-

posed for designing the extremely miniaturized antennas working inside the lossy medium. The radiation efficiencies of the proposed antennas were verified by the numerical simulation and in-vitro and in-vivo measurements, and were much higher than the state-of-the-art implantable antennas. Meanwhile, the wave impedance, radiation performance, and near-field boundary of the antenna inside the lossy medium are systematically investigated.

In general, the path loss models were expected to be used to evaluate and improve the transmission links in all the communication scenarios. Experimental measurements and full-wave numerical simulations were used to build the path loss models for LCP applications, and simplified Cole-Cole models for calculating the relative permittivities and conductivities of human tissues in different frequency bands were proposed to reduce the complexity of the calculation in full-wave simulations. In-body to on-body path loss models in the Ultra-Wideband (UWB) were also built, to achieve high data rate transmission for the WCE application, and the influences of omni-directional and directional on-body antennas on the path loss models were studied.

Highly radiation-efficient implantable antennas are key components of the communication system of LCP, which provides reliable and high-efficiency transmission links. Besides the fact that the miniaturized size of the proposed antennas saves space for the battery in the limited cavity of the pacemaker capsule, it can also extend the lifetime of the pacemaker capsule and avoid the risk of surgery for the patients. In this dissertation, we proposed several new de-

sign concepts and verified the radiation performance of our proposed antenna with the simulated and measured transmission coefficient in homogeneous tissue, an anatomical human model, and a living animal. For the theoretical study, the wave impedance, radiation performance, and boundary between the near-field and far-field of antennas inside the lossy medium are systematically investigated, through which new criterion defining the near-field and far-field boundary and a modified Friis equation for antennas inside the lossy medium were proposed.

For improving the in-body to on-body transmission data rates of WCE applications, compact antipodal Vivaldi antennas working on the UWB were proposed. Without enlarging the size of the antenna, the operating bandwidth was enlarged and the realized gains were improved. To further increase the gain of the on-body antennas, based on the proposed antipodal Vivaldi antenna, two antenna arrays were designed with vertical and horizontal polarization, respectively.

Contents

List of Figures

List of Tables

Acronyms

Notation	Description
AVA	Antipodal Vivaldi Antenna
BER	Bit Error Rate
CPW	Coplanar Waveguide
CSR	Complementary Split-Ring
DRA	Dielectric Resonator Antenna
ERP	Equivalent Radiated Power
ETSI	European Telecommunication Stands Institute
FCC	Federal Communication Commision
FDTD	Finite-Difference Time-Domain
GI	Gastrointestinal
HFSS	High Frequency Structure Simulator
ICD	Implantable Cardioverter Defibrillator
IR	Impulse Radio
ISM	Industrial Scientific and Medical
LCP	Leadless Cardiac Pacemaker
MICS	Medical Implanted Communication Service
NB	Narrow Band

Notation	Description
PCB	Printed Circuit Board
PIFA	Planar Inverted-F Antenna
RO3003	Rogers RO3003^{TM}
RO3010	Rogers RO3010^{TM}
RO6010	Rogers RO6010^{TM}
SAR	Specific Absorption Rate
TSE	Tapered Slot Edge
UWB	Ultra-Wide Band
VNA	Vector Network Analyzer
WBAN	Wireless Body Area Network
WCE	Wireless Capsule Endoscopy
WMTS	Wireless Medical Telemetry Service

Symbols

Notation	Description
ε_0	free space permittivity
ε	permittivity
ε_r	relative permittivity
ε'_r	dielectric constant
ε''_r	loss factor
ε_∞	relative permittivity $f \to \infty$
σ	conductivity or standard deviation
σ_d	displacement conductivity
σ_0	ionic conductivity
ω	angular frequency
τ	relaxation time
f	frequency
δ	skin depth
μ	permeability or mean value of path loss model
μ_0	free space permeability
μ_r	relative permeability
γ	propagation constant
α	attenuation constant
β	phase factor
Z_0	intrinsic wave impedance of free space

Z_{tissue}	intrinsic wave impedance of tissue
E_b	electric field at the observing point
E_0	electric field at the orginating point
d	distance
d_0	reference distance
PL_{PW}	path loss based on plane wave
PL_{Friis}	path loss based on Friis equation
P_r	transmitted power
P_t	received power
$S11$,$S22$	reflection coefficient at the input port of antenna
$S21$	transmission coefficients between antennas
G_r	gain of receiving antenna
G_t	gain of transmitting antenna
λ_{eff}	effective wavelength
$S_{(x,y,z)}(t)$	poynting vector
$E_{(x,y,z)}(t)$	time-domain electric field vector
$H_{(x,y,z)}(t)$	time-domain magnetic field vector
PL	path loss
PL_0	path loss at the reference distance
$N(\mu,\sigma)$	lognormally distributed random variation with mean, μ, and standard deviation σ
n	path loss exponent
Z_{in}	input impedance of antenna
R_{in}	real part of input impedance of antenna
X_{in}	imagnary part of input impedance of antenna
R_r	radiation resistance of antenna
R_L	loss resistance of antenna
L_A	inductance of antenna

L_i	inductance of antenna conductor
C_i	parallel capacitor of antenna
r	propagation distance
a	thickness of insulation layer or radius of sphere surrounding the antenna
Il, $I_M l$	electric and magnetic current moment
λ_{insul}	effective wavelength inside the insulation layer
λ_{tissue}	effective wavelength inside the human tissue
Γ	reflection coefficient on the interface between the insulation layer and surrounding medium
E_E^r	electric field of electric Hertzian dipole at the propagation direction
E_E^θ	electric field of electric Hertzian dipole at the elevation direction
E_E^ϕ	electric field of electric Hertzian dipole at the azimuth direction
H_E^r	magnetic field of electric Hertzian dipole at the propagation direction
H_E^θ	magnetic field of electric Hertzian dipole at the elevation direction
H_E^ϕ	magnetic field of electric Hertzian dipole at the azimuth direction
E_M^r	electric field of magnetic Hertzian dipole at the propagation direction
E_M^θ	electric field of magnetic Hertzian dipole at the elevation direction
E_M^ϕ	electric field of magnetic Hertzian dipole at the azimuth direction
H_M^r	magnetic field of magnetic Hertzian dipole at the propagation direction

H_M^{θ}	magnetic field of magnetic Hertzian dipole at the elevation direction
H_M^{ϕ}	magnetic field of magnetic Hertzian dipole at the azimuth plane
Z_{ant}	wave impedance of antenna versus with the thickness of insulation layer
$Z_E(r)$	wave impedance of electric Hertizan dipole versus with the propagation distance
$Z_M(r)$	wave impedance of magnetic Hertizan dipole versus with the propagation distance
P_0	radiated power of antenna
P_{input}	input power of antenna
η_{lossy}	radiation efficiency of antenna inside lossy medium
E_{E-M}	electric field of helical antenna
H_{E-M}	magnetic field of helical antenna

Chapter 1

Introduction

Research for Wireless Body Area Networks (WBAN) has become popular in recent years, due to its high potential for improving health, providing adjuvant therapy, and extending patients' lives, based on the physiological data collected from different electrically invasive or non-invasive devices inside, or on the human body [1–3]. Many different applications have been proposed and implemented with the assistance of WBAN. Two very specific applications that are areas of cutting-edge medical device research are cardiology and gastroenterology, and two devices were investigated in this study: leadless cardiac pacemaker (LCP) and wireless capsule endoscopy (WCE). This research mainly focused on improving the transmission links of the LCP and WCE communication systems, by building path loss models and designing novel in-body and on-body antennas.

1.1 Motivation and Objectives

1.1.1 Research Motivation

LCP and WCE devices, that are implanted in the human body or swallowed, can monitor the status of different human organs. Each implanted node sends information to the off-body stations and provides treatment to the dysfunctional organ, which can increase patient survival rates and improve health outcomes with easy and fast diagnosis and treatment [4–7]. Therefore, the design of reliable, low power, and highly efficient communication links for these applications is essential.

Characterizing the wave propagation in different communication scenarios of LCP and WCE is an inevitable step to improve the transmission links in the communication systems of implanted devices [8–13]. Scattering and absorption phenomena in the human body, caused by frequency-dependent dielectric properties and the complex structure of human organs, significantly affect the propagation of radio signals through human tissue [14, 15]. The development of mitigation techniques for the high path loss of in-body to in-body, in-body to on-body and in-body to off-body propagation calls for accurate path models and antenna design optimization [16].

To maintain reliable and highly efficient communication among implant devices, especially the in-body to in-body communication of LCP, high radiation efficiency is an essen-

tial characteristic of the implantable antennas. Additionally, for fitting the antenna inside the size-limited implantable medical devices and keeping the Specific Absorption Rate (SAR) as low as possible for patient safety, the in-body antennas should be heavily miniaturized and have high radiation efficiency [17]. Also, the reflection coefficient of in-body antennas should be less sensitive to the detuning effect caused by the differences of electrical properties of human body tissues [18]. For deeply implanted leadless pacemaker capsules, which have to operate inside the heart for 8 to 10 years, longevity is one of the most important requirements.

For the WCE, on-body antennas attached to the skin of the chest and abdomen are utilized to receive signals transmitted from the capsule inside the human body [19–23]. Thus, on-body antennas should be designed with the effect on human tissue taken into consideration. Ultra-wide band (UWB) frequency has high potential as a frequency band for providing high-speed transmission of in-body to on-body communication, so that the real-time images captured by the endoscope capsule can be obtained. However, the large lossy characteristic of the human body during high frequency transmission reduces the possibility of employing an ultra-wide-band antenna in the wireless endoscope capsule [19]. To compensate for the high loss caused by human tissue, the on-body antenna should have high radiation efficiency and gain [22].

1.1.2 Objectives

This work focuses on how to develop stable, low-power consumption, and high-efficiency transmission links for the communication systems of LCP and WCE. To reach the goal, accurate path loss models and high radiation efficiency implantable and on-body antennas will be built and designed. Firstly, the path loss models will be built for all the communication scenarios of LCP and WCE, based on numerical simulation and experimental measurement. The novel implantable antennas with miniaturized volume and high radiation efficiency will then be designed, fabricated, and tested at in vitro and in vivo environments. After that, the theoretical analysis and the numerical simulation will be implemented to discuss the methods for evaluating the radiation efficiency of antennas working inside the lossy medium. The wave impedance, radiation performance, and near-field boundary of the antenna inside the lossy medium will be systematically investigated. Finally, to improve the in-body to on-body communication performance of WCE, compact and high gain on-body antennas and arrays will be designed. These objectives are converted into the following measurable tasks:

1) Developing the low power-consumption and highly efficient transmission links for the communication systems of LCP and WCE.
2) Building the in-body to in-body, in-body to subcutaneous and in-body to off-body path loss models for LCP applications in the narrow frequency bands.
3) Building the in-body to on-body path loss modes for

WCE applications in the ultra-wide band.

4) Designing the miniaturized, highly radiation-efficient implantable antennas for the LCP application and verifying the performance of the designed antenna by in vitro and in vivo measurement.

5) Systematically studying the wave impedance, radiation performance, and near-field boundary of the antenna inside the lossy medium.

6) Proposing the methods of evaluating the radiation performance of antennas implanted in the loss medium.

7) Designing compact and high-gain on-body antennas and arrays for the WCE application.

1.2 Background

1.2.1 Review of Leadless Cardiac Pacemaker (LCP)

Cardiac pacemakers, as the most important and popular implantable devices, can help to detect the phenomenon of cardiac dysfunction and regulate the heart to normal synchronization through connecting the different deeply implanted pacemaker capsules with the subcutaneous control device. For traditional pacemakers, the communication connection and synchronization are created by connecting the several deeply implanted pacemaker capsules to a subcutaneous control unit through wire leads. After decades of pacing technological advancements, leads are usually seen

as the traditional system's weak spot, which might result in breakage, infection, venous blockage, and other complications [24–26].

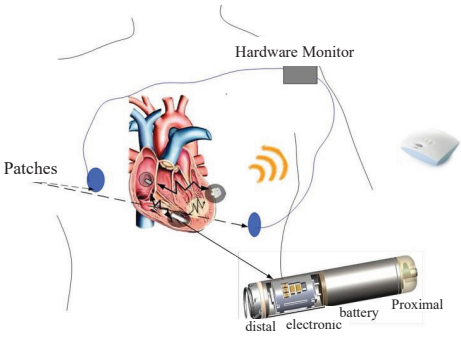

Figure 1.1: Implanted leadless capsule pacemaker [Figure provided by Microport CRM, Paris]

The leadless pacemaker includes a wireless connection in lieu of the lead, which minimizes the risk of infection and is less intrusive for patients. As an alternative to transvenous pacemakers, it has been shown to be both safe and effective in both short- and medium-term follow-up [27–30]. As shown in Fig. 1.1, the LCP consists of distal, electronic, battery and proximal. For the prime monitoring of the heart, at least two leadless pacemaker capsules are required to be deeply implanted in the right atrium and right ventricle respectively and wirelessly synchronize with each other. They will directly communicate with the off-body device or be relayed via the subcutaneously implanted node. There are two possible potential communication modalities: one is that all the capsules work independently as master nodes

having full privileges to communicate with each other and external devices, and another scenario is that an exclusive master capsule acts as the intermediate node for communicating with other slave capsules and external devices.

For the communication technology of LCP, highly reliable and energy-efficient communication links are the most important requirements [31], which implies that the communication system should have a low bit error rate (BER) and high radiation efficiency. Longevity is another important characteristic of a leadless pacemaker that operates inside the heart for 8 to 10 years, thus, the LCP is assumed to have a low-power consumption transceiver and high-radiation efficiency implantable antennas. Since the required communication data rate is no more than 4.8 kbits [32], narrow-band technology is sufficient. To improve the communication performance of LCP applications, path loss models between different capsules should be built. They play a vital role in providing references for the design of communication circuits, evaluating the power consumption of capsules and optimizing the battery's lifetime. Designing antennas with a miniaturized volume to save more space for the battery within the limited capacity of the pacemaker capsule is also significant. As we know, the radiation efficiency of the antenna relates closely to its size; therefore, for deeply implanted devices, miniaturized, high-radiation-efficiency antennas are beneficial.

1.2.2 Review of Wireless Capsule Endoscopy (WCE)

In gastroenterology, Wireless Capsule Endoscopy (WCE), which first appeared in 2000 [33], is a notable invention in the biomedical industry. The ingestible capsule may capture images along its journey through the gastrointestinal (GI) tract after being swallowed. Therefore, it is capable of transmitting real-time biological data from inside the body to external medical tools, advancing noninvasive diagnostics. In the last few years, WCE technology has become popular, replacing the traditional wired endoscopy which may cause complications for medical and sugerical patients [34–36]. Furthermore, the small capsule can reach areas such as the small intestine, where the traditional wired endoscopy cannot detect.

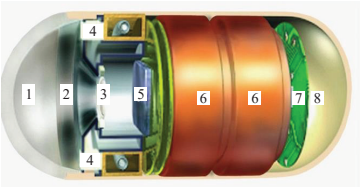

Figure 1.2: PillCam WCE, consisting of (1) Optical dome; (2) Lens holder; (3) Lens; (4) White LEDs; (5) CMOS imager; (6) Battery; (7) Transmitter; (8) Antenna [37].

Fig. 1.2 depicts a PillCam small bowel capsule endoscopy, which consists of a CMOS imager, LEDs, a battery, a transmitter, and an antenna. The CMOS imager, with the assis-

tance of LEDs, captures the pictures when the capsule is going through the stomach and intestines, and then, using the transmitter and implantable antenna, the pictures are transmitted to the off-body or on-body station. Fig. 1.3 depicts another kind of wireless capsule that is also swallowable. It has an optical sensor for the immediate detection of acute bleeding in the esophagus, stomach, and small intestine. This capsule can detect acute bleeding when going through the digestive tract and send real-time information to an outside receiving station, whose working principles are similar to those of WCE.

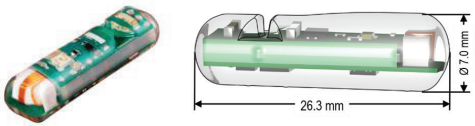

Figure 1.3: HemoPill: Swallowable capsule with optical sensor for the immediate detection of acute bleeding in the esophagus, stomach, and small intestine [38].

The non-invasive examination in a WCE scenario is shown in Fig. 1.4. There is an in-body wireless capsule moving continuously inside the GI tract of the human stomach, wirelessly transmitting the examination data to an on-body antenna. And the received data, pictures or video, can be transmitted to the phone via Bluetooth or WIFI and then remotely shared with the doctor. Normally, the swallowed capsule will stay inside the patient's digestive tract for 8 to

10 hours. Doctors can receive the pictures captured by the WCE even when the patient stays at home.

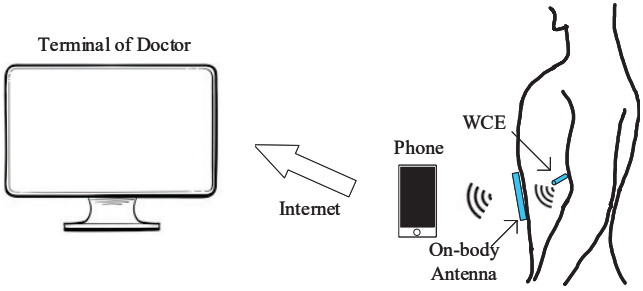

Figure 1.4: Diagram of WCE communication.

There are still many challenges to improving the performance of WCE. Due to the high data rate requirement of this technology, commercial WCE currently operates at narrow frequency bands like the Medical Implant Communication Service (MICS) band and 2.4 GHz ISM band, and the bandwidth restrictions are insufficient for the requirements of high-resolution images for the medically meticulous examination of the gastrointestinal (GI) tract [39–41]. Consequently, UWB is theoretically the greatest feasible frequency band, since it not only gives high-quality pictures but also allows low output power technology, which is a major issue for wireless implanted devices, according to human protection regulatory authorities [42]. It is critical to accurately understand the propagation mechanisms between the in-body and on-body antennas in order to achieve high data rate transmission on UWB. Thus, for the purposes of this study, we built the in-body to on-body path loss

models for the WCE applications and designed the high-gain on-body antenna and antenna array to improve the in-body to on-body transmission.

1.2.3 Potential Frequency Bands

Based on our application scenarios, the LCP and the WCE, the potential frequency bands can be classified into two categories: Ultrawide Band (UWB, 3.1-10 GHz) and Narrow Band (NB) such as Medical Implanted Communication Service (MICS) band (402-405 MHz), Wireless Medical Telemetry Service (WMTS) band (608-614 MHz) and Industrial Scientific and Medical (ISM) bands (867-869 MHz, 2.4-2.5 GHz).

The European Telecommunication Standards Institute (ETSI) has standardized the MICS band, and two types of application fields are listed: one is for communication between an implanted device and an external base station, and the other is for communication between various implanted devices inside the same human body. The maximum power limit is set to -16 dBm equivalent radiated power (ERP) to reduce the risk of interfering with other electric devices in the same band. This means that the maximum field-strength in any direction should be equal to, or lower than, what a resonant dipole would give in its maximum direction at the same distance, fed by a signal of -16 dBm. [43].

The MICS band's low power attenuation within the human

body is its key benefit over the UWB and other higher frequency bands. This makes it potentially useful for in-body communications [44]. The MICS band is extensively exploited by implanted devices for communication with other implanted devices and off-body stations. The MICS band's low power attenuation allows it to propagate further than UWB, but its restricted operating frequency range limits data throughput. The design of the communication system requires miniaturizing the antenna to fit within the implanted device since MICS band antennas are huge.

For narrow band applications, implanted devices may also use the WMTS band, 868 MHz ISM band, and 2.4 GHz ISM band. The 2.4 GHz ISM band, in particular, is now used by a variety of services, including WiFi and Bluetooth, both of which are used by portable smart devices. Because of the widespread use of WiFi and Bluetooth, transmitters that are based on these protocols are fairly simple to implement. Furthermore, the low energy consumption of bluethooth is excellent for implanted devices whose battery life is lengthy. However, this band does not provide any protection against interference from other communication services that operate on the same frequency, which is one of its major drawbacks [44].

The Federal Communication Commission (FCC) defines UWB as the frequencies range from 3.1 GHz to 10.6 GHz with maximum ERP of 74.13 nW/MHz, thus the maximum allowable power of 0.556 mW in the full UWB. European standards provide the low band of UWB between 3.1 GHz and 4.8 GHz and the high band between 6.0 GHz and 10.2

GHz [45]. Due to its lower power attenuation than the high band, the low band is always used for body area communications. UWB offers great promise for high-data-rate applications at short ranges or low-data-rate applications on attenuated channels. UWB further offers antenna miniaturization and decreased power consumption. The primary disadvantage of UWB is its substantial power attenuation inside the human body, which limits communication distance.

1.3 Literature Review

1.3.1 Path Loss Models

Building the path loss models for WCE and LCP can provide references for the design of communication circuits, evaluating the power consumption of capsule and optimizing the battery's lifetime. As we discussed in Section 1.2.3, the operating frequency bands of LCP and WCE are narrow band and ultrawide band, respectively. Thus, the path loss models of these two applications can be classified as narrowband and wideband models.

1.3.1.1 Narrowband Path Loss Models

For the LCP application, the data transmission rate is low, so the narrow frequency band is sufficient and results in lower energy consumption compared with the wideband.

The research of path loss models for the narrow frequency band for in-body communication is summarized as follows. In [46], by modeling and measuring the propagation between implanted devices, channel models of IEEE Standard 802.15.6 in the Body Area Network (BAN) were improved. In order to study RF propagation from medical implants within a human body and establish a statistical path loss model for medical implant communication systems, an immersive visualization environment was developed in [47]. In [48], the author described the experimental measurement and electromagnetic modeling of propagation from 418 MHz and 916.5 MHz sources placed in the human vagina. An on-body propagation channel for 4.5 GHz was measured with a specific activity of a body in [49]. Different body processes' effects on fading were observed and statistically modeled. In [50], for a 2360 MHz on-body to on-body channel, the impact of gender and body shape was shown. The findings demonstrated that small-scale fading that conforms to the Rice distribution is caused by involuntary movements as well as breathing. In [51], the propagation channel between two 2.45 GHz half-wavelength dipoles near a human body was discussed. In a multipath scenario, propagation measurements were conducted on actual persons. The signal propagation around the surface of the body at 915 MHz and 2.45 GHz (ISM bands) was examined in [52]. Wearable wireless low-cost commercial modules and low-profile annular ring slot antennas were used as transceivers to measure the on-body path loss models in [53].

In [54], the belt-to-head and belt-to-wrist propagation models were derived using monopole, loop, dipole, and inverted

F-antennas. The authors observed that short-term fading is Rician and log-term is lognormal. Biotelemetry and in-body radio propagation at 402 MHz, 868 MHz, and 2.4 GHz are examined numerically and experimentally in [55]. The findings suggest that 402 MHz is excellent for wireless implants and that the ISM band 2.4 GHz may be utilized for body-worn medical sensors to transmit in-body data to nearby locations. In [56], the author measured the on-body propagation around the body surface and in-body propagation through tissue at 403 MHz and 2.45 GHz and found that in-body path loss is more than that of on-body. In [57], the radiation properties of wireless sensors placed on various human organs and various inhomogeneous digital phantoms at 403 MHz and 868 MHz were investigated by numerical simulations based on FDTD. The study revealed that the location significantly affects wireless sensor performance, with body curvature potentially enhancing antenna directivity. Taking into account human body curvature, including human models with organs properties in [58], the path loss models of in-body to on-body and in-body to in-body at 402 MHz, 868 MHz, and 2.4 GHz are investigated by numerical simulation based on FDTD and phantom measurement.

1.3.1.2 Wideband Path Loss Models

Wideband path loss models may be used in WCE applications as a guide for the design of transverse, in-body, and on-body antennas to achieve high data rate communication. Many studies of wideband path loss channel models have been conducted. In [59], the propagation of UWB

signals through human tissues in the 0.1-1 GHz and 1-6 GHz frequency bands was simulated and studied based on the numerical anatomical human body. A statistical model for UWB propagation channels inside the human chest in the 1-6 GHz frequency range by including the frequency-dependent attenuation is extended in [60]. Based on FDTD method, the wireless link between the inside and outside of a human chest was studied with the disc dipole antennas [61]. In [62], a spatial diversity reception technique was employed to improve the communication performance between in-body and on-body devices at UWB. To capture the effects of blood circulation, respiration, and temperature gradients of a living subject, in [63], the author performed UWB channel measurements within 1-6 GHz on two living porcine subjects. In [64], radio propagation around the body at 3-10 GHz was examined using parallel FDTD. Simulation and measurement were in a typical hospital environment. Based on in-vivo measurements made in the abdominal cavity, the in-body to on-body and in-body to off-body path loss models within the range of 3.1 GHz to 8.5 GHz were retrieved in [65]. Additionally, the correction factors to change phantom-based results to more accurate path loss values are offered by contrasting them with in-vivo-based measurements. In [66], the arm motions and background office noise are taken into account when developing the log-normal path loss models based on measurements of electromagnetic waves passing close to the body. The frequency dependency of the scattering component has also been examined together with the frequency-dependent path loss model for ultrawideband implant applications in [67].

1.3.2 In-Body Antenna Design

The design of antennas working inside the human tissue with high permittivity and conductivity is very challenging. Because of the electrical characteristics of human tissue, the design concepts for in-body antennas differ from those for antennas in free space. It has been found that it is not only the high permittivity of human tissue that gives the shorting fact to the antennas but also the high conductivity. In particular, high water-content tissues such as the heart, blood, muscles, etc., distort the field distribution of the in-body antenna. Thus, the evaluation methods for the antenna performance in free space cannot be directly applied to the in-body antenna. For example, the radiation pattern and efficiency of the antenna inside the lossy medium need to be redefined [18, 68–73]. Insulation is also one of the most important factors which should be considered in the design of in-body antenna because the thickness and electric property of it influence the near field distribution of implantable antenna [74–76]. And the radiation pattern of an implanted antenna cannot be defined as it is in free space because it also depends on the dimensions and electric properties of surrounding media, not only the antenna itself [68].

1.3.2.1 Narrow Band In-Body Antenna

The antennas in the leadless capsules of LCP application are deeply implanted inside the heart, which is a tissue consisting of high water-content tissue with large permittivity and conductivity. Since the antenna only necessitates a

low data rate, its operating frequency can be confined to a narrow band. Compared with the antenna working in free space, the special working environment of in-body antenna changes the design principle significantly.

Many studies have been conducted. In [77], an implantable planar inverted-F antenna (PIFA) was designed and analyzed inside the muscle tissue.The antenna's path and ground plane were designed with a curvature, creating a three-dimensional structure that aligns with the capsule's curvature. A compact stacked planar antenna working on the MICS band was proposed and fabricated in [78]. In addition, the antenna's resonance frequency and radiation performance were examined inside a head model. In [79], to miniaturize the size of the antenna, a kind of high permittivity substrate, with 30 of relative permittivity, was employed. The antenna was placed in a simplified biological tissue model consisting of bone, muscle, fat, and skin; then, the 1g-SAR distribution, resonant frequency, and radiation pattern were analyzed. The meandered PIFA structure was utilized to design the implanted RFID tag antenna operating at 868 MHz (ISM band) [80]. The wave propagation between the off-body reader and the implanted tag was analyzed in free space and in a scattered environment. The authors of [81] proposed an implanted H-shaped cavity slot antenna for short-range wireless communication. The antenna was designed to operate on the ISM band (2.45 GHz) and investigated by using finite-difference time-domain (FDTD) calculations. In [82], the multilayer helical antenna was applied to miniaturize the size of the antenna to a diameter of 12 mm for 2.4 GHz ISM band ingestible capsule endoscope

systems. A folded structure [83] was employed to design an implant compact folded antenna of 20.3 mm × 0.8 mm × 0.8 mm operating at one of the UHF bands (951-956 MHz).

In [84], an electrically coupled loop antenna was proposed which was dual of PIFA. Further, the proposed antenna was utilized for implanted devices inside the human body as a good candidate for miniaturized and high radiation efficiency antenna in [85]. A dual-band scalp-implantable antenna is proposed in [86], in which the antenna works at 915 MHz and 2450 MHz and has a small volume (8 mm × 6 mm × 0.5 mm = 24 mm^3) with a slotless and a vialess ground plane. In [87], a coplanar waveguide (CPW) fed patch antenna is proposed and works at 2.4-2.5 GHz with the circular polarization inside the skin and muscle. The main radiation part of the antenna is a meandered central strip, and the asymmetric square slots are utilized to generate phase conditions for right-hand circularly polarized radiation. In [88], a triple band implantable antenna is proposed, which operates at 902-928 MHz, 2400-2483.5 MHz, and 1824-1980 MHz. The size of the proposed antenna is 21 mm^3 (7 mm × 6 mm × 0.5 mm) and consists of a meandering radiating patch, an open-end ground slot, and a shorting pin between the ground plane and radiating patch. A dual-band (MICS and ISM bands) implantable complementary split-ring (CSR) antenna is proposed in [89], and the antenna is fabricated on a grounded RO3010 and with 14 mm × 14 mm × 1.27 mm in size. In [90], a circularly polarized implantable antenna operating at 902-928 MHz is presented and the size of the antenna is $pi \times (6 \text{ mm})^2 \times 1.27$ mm. The structure of the antenna is an extended ring with meandered lines.

In [91], a small circular polarization path antenna with the capacitive loading was designed, and the capacitive loading was used to reduce the size to 10 mm × 10 mm × 1.27 mm working at 2.4-2.48 GHz. A dual band antenna (402 MHz MICS band and 2.45 GHz ISM band) was designed with differential feeding and 22 mm × 23 mm × 1.24 mm in size [92].

1.3.2.2 Wideband In-Body Antenna

Wideband implanted antennas are required for the WCE application to provide high data rate connectivity and real-time, high-quality picture transmission. In [93], by using dielectric loading technology, a capsule-shaped slot antenna was developed with a larger matching bandwidth and a smaller overall dimension. The proposed design has an operational bandwidth of 3.5 GHz to 4.5 GHz. It was suggested to use a conformal trapezoid strip excited broadband hemispherical dielectric resonator antenna (DRA) in [94]. The authors exploited the UWB transmission loss characteristics in human tissue, and analyzed the performance of in-body to on-body communication. One of the most compelling advantages of a UWB implanted antenna is its potential to enhance the transmission data rate. In [95], the authors used impulse radio (IR) in the near-field to achieve a 750 Mbps data rate based on an uniplanar printed antenna. In order to increase the transmission data rate in [96], a UWB transmitter diversity antenna was developed. Based on phantom and in-vivo tests, a projected outage rate of 0.01 and a range of 15 cm in a typical body environment may theoretically be accomplished with a 7 dB increase

in signal-to-noise power ratio. In [97], a dual-wideband implantable antenna was proposed, whose measured -10 dB bandwidths are 56% (278 MHz) for the MedRadio and 33% (870 MHz) for the ISM bands, respectively. In [98], a CPW-fed, wideband dual-ring slot antenna was propsoed with the bandwidth of 57% (2-3.5 GHz). By introducing a metamaterial (MTM) array with very large epsilon behaviorAnd, a 3 dB gain enhancement was achieved. In [99], four flexible, polarization-diverse UWB antennas are proposed for an implantable neural recording system. The bandwidth of the proposed antennas is from 2 GHz to 11 GHz and there are two different dimensions for the single- and dual-polarization antennas: 12 mm $\times$ 12 mm and 10 mm $\times$ 9 mm, respectively. In [100], a flexible antenna operating from 3.1 GHz to 10.6 GHz with an overall size of 17 mm $\times$ 14 mm $\times$ 1.07 mm was proposed and the antenna is compatible for use with off-body, on-body as well as in-body applications.

1.3.3 On-Body Antenna Design

When it comes to receiving data transmitted from implanted devices, such as those used in WCE applications, wearable on-body antennas are an absolute necessity. In [101], for 3.1 GHz to 10.6 GHz IR-UWB systems, a new small microstrip-fed printed monopole antenna was introduced and studied. The transmission scenarios in which many antennas were positioned on the body were evaluated and compared, and the findings revealed great path gain. A dual-band coplanar patch antenna was integrated with an electromagnetic band gap substrate in order to improve the antenna gain

while also lowering the amount of radiation that entered the body, as described in [102]. The antenna worked in the 2.45 GHz and 5 GHz bands and was constructed using regular clothing. By integrating the antenna with a band gap array, the radiation penetrating the body was significantly reduced by nearly 10 dB, while simultaneously achieving an increase in gain of 3 dB. For medical diagnosis in the 0.5 GHz to 2 GHz range, a compact double-layer Bowtie antenna based on a folded construction with meandering microstrip lines at the bottom was designed [103]. This antenna demonstrated a significant potential for usage in the medical diagnosis of stroke, breast cancer, and water accumulation detection in human bodies thanks to features including a very small size, very low operational frequency, and a high front-to-back ratio. In [104], The authors evaluated and reviewed a variety of UWB on-body slotted path antennas, and they suggested an improved model with a slot loaded with circles and fed by a fork-shaped microstrip line. In order to increase the communication range of implantable medical devices, a dual-band patch antenna was proposed for integration into on-body repeater devices. These devices were designed to receive and retransmit weak signals from implantable medical devices (MedRadio band, 401-406 MHz) to monitoring/control devices placed at a greater distance (ISM 2400-2480 MHz) [105]. In [106], for on-body applications, a one-wavelength loop antenna fed by an inductively linked loop was developed. The antenna was matched at 880-940 MHz and printed on a PVC substrate. In order to meet the specifications of RFID applications, the radiation and matching performance of the developed on-body antenna were simulated on the human body. A surface wave antenna, consisting of an artificial ground plane ex-

cited by a center-fed circular patch, was presented [107]. The input-match frequency band was around 2.45 GHz and the radiation pattern was monopole-like. In [108], based on a novel half-diamond-shaped HMSIW architecture, a dual-band wearable antenna comprised of textile materials and brass eyelets was described. There was extremely high agreement between models and experiments for impedance matching and radiation performance in free space in the 2.4 GHz and 5.8 GHz ISM bands.

1.4 Overview of the Dissertation

The Dissertation is organized into six chapters. The following is how the dissertattion is organized:

Chapter 1 introduces the motivation and objectives of our work and provides a brief background on two biomedical implantable devices: the WCE and LCP. Moreover, a literature review of previous research on path loss channel models, in-body antennas and on-body antennas is provided.

Chapter 2 describes the theoretical analysis of the electromagnetic properties of human body tissues and the characteristics of wave propagation inside human body tissues. The in-body to in-body, in-body to subcutaneous and in-body to off-body path loss models for the LCP applications are built. It also shows the in-body to on-body channel models for the WCE application.

Chapter 3 proposes novel miniaturized loop antennas for implantable applications. The design principle is discussed, and the effects of the thickness of the insulation layer and different human tissues are investigated. The proposed antennas are also integrated with the models of leadless pacemakers to study the influence of the pacemakers on the proposed antenna. The performance of the antenna is verified with full-wave simulation in the antomical model, in-vitro phantom measurement and in-vivo animal experiment.

Chapter 4 systematically investigates the wave impedance, radiation performance, and near-field boundary of the antenna inside the lossy medium. The wave impedance of electric and magnetic dipoles inside the lossy medium is discussed, and the influence of the thickness of the insulation layer on the half-wave dipole inside the lossy medium is also studied. The modified concepts for evaluating the radiation performance of antennas inside the lossy medium are proposed, and the methods to evaluate the radiation efficiency of antennas inside the lossy medium are provided. The equation for evaluating the link budget between antennas inside the lossy medium is summarized and verified, based on the simulation and measured results of our proposed antennas.

Chapter 5 provides the designed compact antipodal Vivaldi antenna, and antipodal Vivaldi antenna arrays, all of which are working at the low part of UWB and are utilized as on-body antennas for the WCE application.

Chapter 6 summarizes and concludes the dissertation as well as suggesting future work.